Geophysical Research Letters

RESEARCH LETTER
10.1029/2019GL082111

# Van Allen Probes Observations of Chorus Wave Vector Orientations: Implications for the Chorus-to-Hiss Mechanism

**D. P. Hartley[1], C. A. Kletzing[1], L. Chen[2], R. B. Horne[3], and O. Santolík[4,5]**

[1]Department of Physics and Astronomy, University of Iowa, Iowa City, IA, USA, [2]Department of Physics, University of Texas at Dallas, Richardson, TX, USA, [3]British Antarctic Survey, UK, [4]Department of Space Physics, Institute of Atmospheric Physics, Prague, Czech Republic, [5]Faculty of Mathematics and Physics, Charles University, Prague, Czech Republic

**Key Points:**
- On a global scale, chorus waves rarely exist with the wave vector orientation required to access the plasmasphere and evolve into hiss
- Only in a small region on the duskside, close to plumes, can a substantial fraction of chorus waves propagate into the plasmasphere
- This spatial limitation qualitatively indicates that chorus waves may only contribute a small fraction of the plasmaspheric hiss wave power

**Correspondence to:**
D. P. Hartley,
david-hartley@uiowa.edu

**Citation:**
Hartley, D. P., Kletzing, C. A., Chen, L., Horne, R. B., & Santolík, O. (2019). Van Allen Probes observations of chorus wave vector orientations: Implications for the chorus-to-hiss mechanism. *Geophysical Research Letters*, *46*, 2337–2346. https://doi.org/10.1029/2019GL082111

Received 17 JAN 2019
Accepted 22 FEB 2019
Accepted article online 27 FEB 2019
Published online 6 MAR 2019



**Abstract** Using observations from the Van Allen Probes EMFISIS instrument, coupled with ray tracing simulations, we determine the fraction of chorus wave power with the conditions required to access the plasmasphere and evolve into plasmaspheric hiss. It is found that only an extremely small fraction of chorus occurs with the required wave vector orientation, carrying only a small fraction of the total chorus wave power. The exception is on the edge of plasmaspheric plumes, where strong azimuthal density gradients are present. In these cases, up to 94% of chorus wave power exists with the conditions required to access the plasmasphere. As such, we conclude that strong azimuthal density gradients are actually a requirement if a significant fraction of chorus wave power is to enter the plasmasphere and be a source of plasmaspheric hiss. This result suggests it is unlikely that chorus directly contributes a significant fraction of plasmaspheric hiss wave power.

**Plain Language Summary** Plasmaspheric hiss waves are typically observed inside a high-density region of geospace known as the plasmasphere. Chorus waves are typically observed at higher altitudes, beyond the plasmasphere region, where the density is substantially lower. Despite the differences between these two wave types, it has been proposed that chorus waves may propagate in such a way that they enter the plasmasphere, where they become a source of plasmaspheric hiss. However, this mechanism can only occur if chorus waves have a specific set of initial conditions. In this study, we find that chorus waves are rarely observed with these required conditions. Only in a spatially limited region close to the edge of plasmaspheric plume structures, where chorus wave power is typically weaker, do we observe a significant fraction of chorus waves that exist with the conditions required to propagate into the plasmasphere. This result qualitatively indicates that chorus waves may not be a substantial source of plasmaspheric hiss.

## 1. Introduction

The dynamics of Earth's outer electron radiation belt are, in part, driven by interactions with a diverse array of electromagnetic waves (e.g., Thorne, 2010; Xiao et al., 2009, 2010, 2015). Two waves that play critical roles are whistler-mode chorus waves (e.g., Bortnik & Thorne, 2007; Summers et al., 2007) and plasmaspheric hiss (e.g., Lyons et al., 1972; Lyons & Thorne, 1973; Selesnick et al., 2003; Thorne et al., 2013). These two wave modes are typically separated by the plasmapause, with hiss occurring in the high-density, plasmasphere (e.g., Hartley, Kletzing, De Pascuale, et al., 2018; Meredith et al., 2004; Thorne et al., 1973), and chorus waves occurring in the lower density region beyond this boundary (e.g., Burtis & Helliwell, 1969; Meredith et al., 2003). Chorus waves occur at frequencies from ~ 100 Hz up to several kHz (e.g., (Gurnett & O'Brien, 1964; Xiao et al., 2017). They are typically observed as coherent burst emissions that scale with the electron cyclotron frequency, $f_{ce}$, in the equatorial source region, with characteristic frequencies between 0.05 and 0.90 $f_{ce}$. By comparison, plasmaspheric hiss is a more broadband emission with frequencies ranging from several kHz down to ~ 30 Hz (Chen et al., 2014; Li et al., 2013; Malaspina et al., 2017; Ni et al., 2014). Despite the apparent differences between these two whistler-mode waves, ray tracing studies suggest that there may be a causal link between them (Bortnik et al., 2008; Chum & Santolík, 2005; Santolík et al., 2006).

It has been proposed that the lower portion of the chorus frequency band can propagate to high latitudes and low altitudes, enter the plasmasphere, and evolve into plasmaspheric hiss (Bortnik et al., 2008; Chum & Santolík, 2005; Santolík et al., 2006). Observations have supported this theory, with multi-spacecraft measurements of enhancements in chorus wave power within approximately three Earth radii, $R_E$, of the plasmapause correlating with enhancements in plasmaspheric hiss observed between 1 and 7 s later (Bortnik et al., 2009; Wang et al., 2011). Further investigation revealed chorus at larger radial distances, ~10 $R_E$, could be a source of plasmaspheric hiss with observed time delays of 5–8 s, consistent with propagation times predicted by ray tracing (Li et al., 2015). Agapitov et al. (2018) showed substantial correlation between chorus and hiss wave power observed by the Time History of Events and Macroscale Interactions during Substorms (THEMIS) mission, occurring most frequently in the post-noon sector, with ~20% of chorus observed between 12 and 16 in magnetic local time (MLT) being well correlated with hiss waves observed inside of the plasmasphere immediately afterward. Through extensive modeling efforts it has also been demonstrated that this chorus-to-hiss mechanism could reproduce the frequency range, wave power, and the spatial structure of plamsaspheric hiss (e.g., Chen, Bortnik, et al., 2012a, 2012b; Chen, Li, et al., 2012; Meredith et al., 2013).

From ray tracing simulations (e.g., Bortnik, Chen, Li, Thorne, & Horne, 2011; Bortnik, Chen, Li, Thorne, Meredith, & Horne, 2011; Bortnik et al., 2016; Chum & Santolík, 2005) it is apparent that in order for chorus waves to access the plasmasphere, they must exist with a specific wave vector orientation. The polar wave vector angle, $\theta$, is defined as the angle between the wave vector and Earth's magnetic field vector, whereas the azimuthal wave vector angle, $\phi$, is defined as the angle of the wave vector around the background magnetic field with respect to the anti-Earthward direction. When the magnetospheric plasma is represented by a diffusive equilibrium density model with no longitudinal dependence and a superimposed plasmapause, an oblique polar wave vector angle, between 30° and 60°, and an azimuthal wave vector angle oriented approximately toward the Earth is required in order for a chorus wave to enter the plasmasphere (e.g., Bortnik et al., 2008, 2009; Hartley, Kletzing, Santolík, et al., 2018; Zhou et al., 2016). Chen, Bortnik, et al. (2012a) identified the key parameters for chorus to enter the plasmasphere as follows; source locations within ~3 $R_E$ of the plasmapause, wave vectors oriented toward Earth with polar angles between 30° and 60°, and wave frequencies of $f/f_{ce}$ <0.3. Implementing an asymmetric density model with azimuthal density gradients to account for the storm time magnetosphere and the duskside plasmaspheric plume/bulge (Chen et al., 2009) permits chorus waves with a broader range of wave vector orientations to gain access to the plasmasphere, but only close to the edge of the plume.

While numerous studies have shown that this chorus-to-hiss process is possible, and even consistent with satellite observations, one missing piece is the direct measurement of chorus waves with the initial conditions required to penetrate into the plasmasphere. In a previous simulation by Chen, Bortnik, et al. (2012a), it was assumed that the equatorial wave normal distribution was centered on the background magnetic field direction with an angular width of 45° in the meridian plane. This assumed distribution has not been observationally verified. Only now, with systematic observations from the Electric and Magnetic Field Instrument and Integrated Science (EMFISIS) suite (Kletzing et al., 2013) housed on the Van Allen Probes dual-satellite mission (Mauk et al., 2012), is it possible to conclusively test whether chorus waves with these initial conditions exist in the geospace environment and determine whether they are observed frequently enough, and with sufficient power, to be a significant source of plasmaspheric hiss.

## 2. EMFISIS Observations

EMFISIS routinely measures the wave magnetic and electric field every 6 s, using onboard calculation of six-dimensional spectral matrices from 500-ms waveform captures. From this survey data, the singular value decomposition (SVD) method is used to calculate wave propagation characteristics (Santolík et al., 2003). Since whistler-mode chorus waves are typically coherent, right-handed, and circularly polarized, data are only included in the present study if both the polarization and ellipticity are greater than 0.5 (Santolík et al., 2002). Since only the magnetic field is used for determining these values, this analysis is not subject to antenna sheath impedance effects associated with electric field observations (e.g., Hartley et al., 2015, 2016, 2017). The spacecraft must be located outside of the plasmasphere for waves to be identified as chorus (density below $10 \times (6.6/L)^4$ or 30 $cm^3$, whichever is smaller, as in Bingham et al., 2018; Hartley et al., 2015, 2016; Li et al., 2014).

To ensure sufficient power for reliable wave normal angle estimates, observations are restricted to periods when the power spectral density is greater than $10^{-7}$ $nT^2/Hz$, ensuring a signal of at least 10 times instrument background levels. Since SVD methodology assumes the presence of a single plane wave, a threshold of planarity >0.6 is imposed, allowing for a maximum of 10% of total power, and 16% of power with respect to the largest axis of the 3-D polarization ellipsoid, outside of the polarization plane (e.g., Hartley, Kletzing, Santolík, et al., 2018). These high-planarity, more intense chorus waves account for over 90% of the total chorus wave power observed in the survey data captured by the Van Allen Probes satellites over the mission duration. That is, the cumulative chorus wave power after imposing the planarity and power spectral density thresholds divided by the cumulative chorus wave power prior to imposing these thresholds yields a value greater than 0.9. This is due to the fact that more intense chorus waves are usually planar. As such, very little wave power is neglected by imposing these additional criteria. It should be noted that due to the Van Allen Probes orbit, EMFISIS data are limited to ±20° magnetic latitude.

The polar and azimuthal wave vector angles ($\theta$ and $\phi$, respectively) are direct outputs from the SVD analysis. As such, it is possible to perform a statistical analysis of wave vector orientations to determine how frequently, and with how much power, chorus waves occur with the conditions required to enter the plasmasphere and evolve into plasmaspheric hiss.

## 3. Results and Discussion

Ray tracing is used to determine the initial conditions required for chorus waves to propagate into the plasmasphere using a cold plasma medium in the HOTRAY program (Horne, 1989). If a wave trajectory does not enter the plasmasphere within 2 seconds, it is no longer traced and considered unable to enter the plasmasphere at any subsequent times. This 2-s cutoff is based on modeling with explicitly calculated damping rates shown in Bortnik, Chen, Li, Thorne, and Horne (2011), where for a source location at 6 $R_E$, ray lifetimes are less than 2 s for waves that do not enter the plasmasphere and greater than 2 s only for waves that do propagate into the plasmasphere. Since the current study only includes data for L <6.5, and propagation times are generally shorter for lower L shells, this 2-s cutoff is deemed appropriate. In the simulation presented here, a diffusive equilibrium density model is used (Angerami & Thomas, 1964; Inan & Bell, 1977; Kimura, 1966) with a plasmapause fixed at 4.5 $R_E$ and the same parameter values implemented and described in section 2.2 of Bortnik, Chen, Li, Thorne, and Horne (2011), but without density ducts. Waves are injected at a radial distance of 6 $R_E$ at magnetic latitudes of 0°, 10°, and 20° (matching the range sampled by EMFISIS) with a wave frequency of 0.20 $f_{ce}$ for the full range of possible wave vector orientations from 0° to 90° in $\theta$ and −180° to 180° in $\phi$ in 5° intervals. These ray tracing results are shown in the meridional plane in Figure 1a with the plasmasphere shaded in gray. The equatorial electron density profile, $n_e$, is also provided. It is evident that the majority of wave vector orientations do not result in the wave trajectory entering the plasmasphere (red ray paths). However, there are a subset of wave vector orientations that propagate in such a way that they enter the plasmasphere at high latitude, and can potentially be a source of plasmaspheric hiss (green ray paths). Figure 1b summarizes the initial wave vector orientations that can, and cannot, enter the plasmasphere, with the polar wave vector angle, $\theta$, shown in the radial direction and the azimuthal wave vector angle, $\phi$, shown in the tangential direction, as indicated by the yellow arrows. If a wave can access the plasmasphere from any one of the source latitudes, this area in $\theta - \phi$ is shaded in green, whereas if the wave cannot access the plasmasphere from any of the source latitudes it is shown in red.

Figure 1c shows a probability distribution function (PDF) of chorus wave occurrences between $L = 5.5$ and 6.5 in a 0.05 $f_{ce}$ wide frequency band centered at 0.20 $f_{ce}$ as a function of polar and azimuthal wave vector angles. Data from all MLTs and all sampled magnetic latitudes are included in this analysis. The vast majority of wave vectors are oriented with a component in the anti-Earthward direction (85% of observations) with similar results obtained for all studied L shells and frequency bands. This structure is a consequence of propagation, assuming a field-aligned wave vector in the equatorial source region and wave vectors inclining anti-Earthward during propagation. A bimodal distribution is apparent in the polar direction with a primary population of waves with $\theta < 40°$ and a significantly smaller secondary population of very oblique waves, as in Li et al. (2016). Figure 1d is in the same format but shows the PDF of wave power observed in this frequency band. The majority of the wave power is contained in the waves that are approximately field aligned.

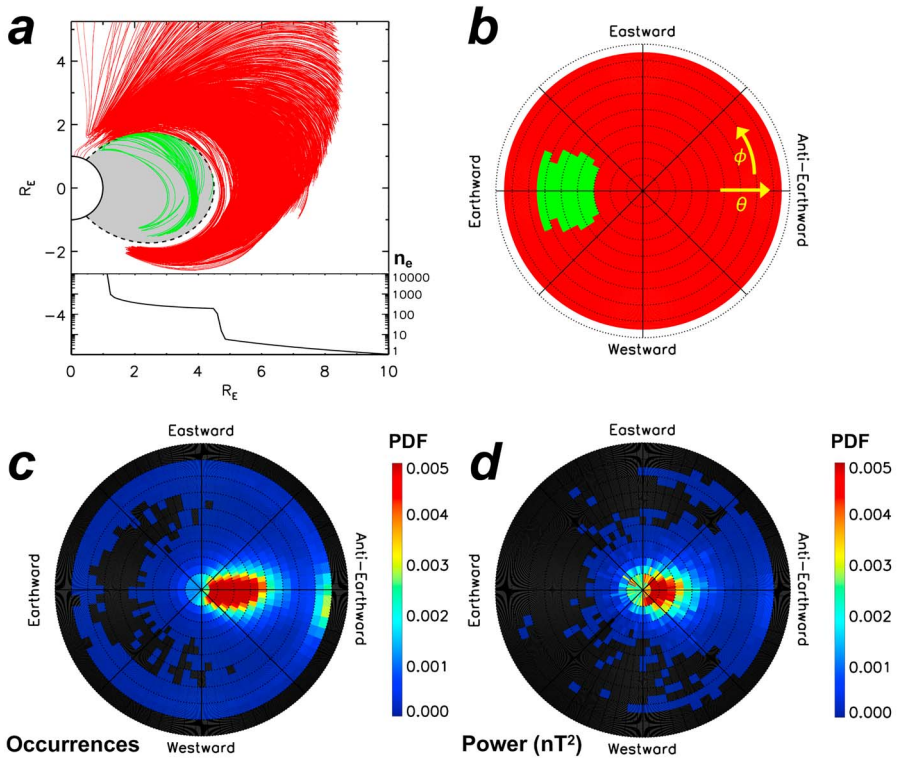


| e | Occurrences | | | | Wave Power (nT²) | | | |
|---|---|---|---|---|---|---|---|---|
| | L = 5 | | L = 6 | | L = 5 | | L = 6 | |
| 0.10 $f_{ce}$ | 0.37% | 178,178 | 0.16% | 694,535 | 0.35% | 37 nT² | 0.15% | 122 nT² |
| | | 664 | | 1,128 | | 0.13 nT² | | 0.19 nT² |
| 0.15 $f_{ce}$ | 0.32% | 107,497 | 0.13% | 479,327 | 0.49% | 62 nT² | 0.098% | 165 nT² |
| | | 348 | | 613 | | 0.31 nT² | | 0.16 nT² |
| 0.20 $f_{ce}$ | 0.31% | 98,601 | 0.12% | 368,060 | 0.56% | 72 nT² | 0.094% | 180 nT² |
| | | 303 | | 447 | | 0.41 nT² | | 0.17 nT² |

**Figure 1.** (a) Propagation paths of 0.20 $f_{ce}$ waves and the equatorial density profile. (b) Wave vector orientations that do (green), and do not (red), enter plasmasphere. Probability distribution functions (PDF) of 0.20 $f_{ce}$ wave (c) occurrences, and (d) wave power, at $L = 6$ as a function of $\theta$ and $\phi$. (e) Table containing percentage of occurrences and wave power that can enter plasmasphere (left). Also listed are the total occurrences/power (top right), and the occurrences/power that can enter the plasmasphere (bottom right).

Comparison between Figures 1b, 1c, and 1d allows for the determination of both the number of occurrences and the wave power that occur with the conditions required to gain access to the plasmasphere. This information is contained in Figure 1e: percentage of occurrences and wave power that can access the plasmasphere (left columns), total occurrences (top) and the occurrences that can access the plasmasphere (bottom), total wave power (top), and the wave power that can access the plasmasphere (bottom). It is found that of 368,060 chorus waves observed at 0.20 $f_{ce}$ and $5.5 < L < 6.5$, only 447, or 0.12% exist with the wave vector orientation required to enter the plasmasphere. It is also found that these waves contain only 0.17 nT$^2$, or 0.094% of the total chorus wave power of 180 nT$^2$ observed under these conditions. This analysis is repeated for different wave frequencies (0.10, 0.15, 0.20 $f_{ce}$) and source locations ($L = 5, 6$). Similar results are obtained under all conditions with the maximum percentage of occurrences being 0.37% for 0.10$f_{ce}$ waves and a source location of $L = 5$ and the maximum wave power percentage being 0.56% for 0.20 $f_{ce}$ waves and a source location of $L = 5$.

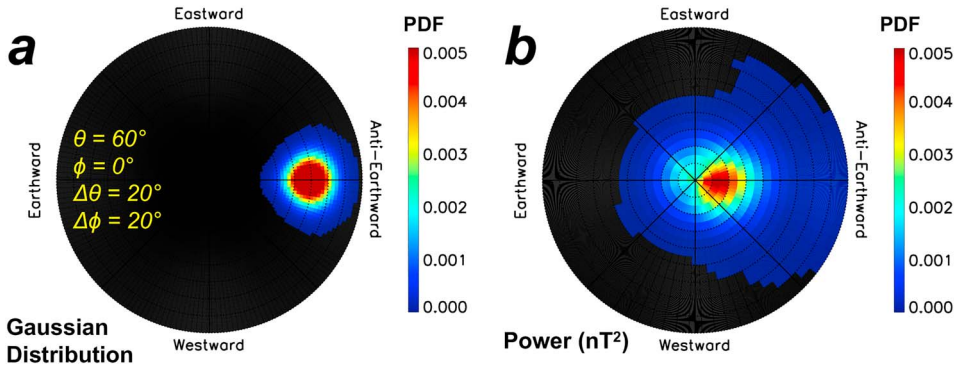


**c**

| | Wave Power (nT²) | | | |
|---|---|---|---|---|
| | L = 5 | | L = 6 | |
| 0.10 $f_{ce}$ | 0.91% | 37 nT² | 0.53% | 122 nT² |
| | | 0.34 nT² | | 0.65 nT² |
| 0.15 $f_{ce}$ | 0.95% | 62 nT² | 0.38% | 165 nT² |
| | | 0.59 nT² | | 0.64 nT² |
| 0.20 $f_{ce}$ | 0.87% | 72 nT² | 0.31% | 180 nT² |
| | | 0.63 nT² | | 0.56 nT² |

**Figure 2.** (a) Example of Gaussian angular probability distribution function centered at $\theta = 60°$ and $\phi = 0°$ with an angular width of $\Delta\theta = \Delta\phi = 20°$. (b) Probability distribution function of wave power for 0.20 $f_{ce}$ chorus at $L = 6$ after a distribution width of $\Delta\theta = \Delta\phi = 20°$ has been applied. (c) Percentages of wave power that can enter plasmasphere after modeling the distribution angular width (left). The wave power in each distribution (top right) and the wave power that can access the plasmasphere (bottom right).

Thus far in this analysis, it has been assumed that the observed power spectral density occurs with a single wave vector orientation based on the $\theta$ and $\phi$ values from the SVD analysis. In actuality, the power spectral density is a distribution over a range of wave vector orientations, peaked about the SVD inferred direction (Santolík et al., 2003). This distribution width can be incorporated into the analysis by modeling the power spectral density as a Gaussian distribution with a polar width (full width half maximum, FWHM), $\Delta\theta$, and an azimuthal FWHM, $\Delta\phi$, where the integral over the full distribution is equal to the power spectral density observed by the spacecraft at each time instance. Here the wave planarity is used as a proxy for estimating the angular width of this distribution. The mean and median planarity of waves included in this study are 0.741 and 0.739, respectively. Santolík et al. (2003) computed that for $Z$-mode waves, a planarity of 0.7 yields an angular width of around 20°. Similar analysis by Taubenschuss and Santolík (2019) has been done for whistler-mode waves under the influence of noise and shows that a planarity of 0.7 corresponds to an uncertainty in theta of 20° for approximately five averaged spectral matrices. As such, $\Delta\theta = \Delta\phi = 20°$ is used here as a reasonable approximation.

Figure 2a shows an example of this angular distribution for SVD determined values of $\theta = 60°$ and $\phi = 0°$. A distribution of this type is generated for each chorus wave observation, with the peak centered on the SVD wave normal direction at each time instance. Since the integral of this distribution over all $\theta$ and $\phi$ is equal to unity, the power spectral density associated with each chorus wave observation is now scaled by this distribution in order to incorporate the angular width into the analysis. These power spectral density distributions for each time instance are then used to recreate the PDFs of magnetic field wave power in order to establish the impact of this distribution width on the amount of wave power that can access the plasmasphere.

Applying this distribution width to the magnetic field power spectral density observations and computing the wave power that exists with the $\theta$ and $\phi$ values required to access the plasmasphere yields the results

shown in Figure 2b for the same conditions shown in Figure 1 ($0.20\,f_{ce}, L = 6$). By including the distribution width, the percentage of observed chorus wave power that can access the plasmasphere increases from 0.094% to 0.31%.

This analysis is repeated for all frequencies (0.10, 0.15, 0.20 $f_{ce}$) and source locations ($L = 5, 6$), with the results provided in Figure 2c. For completeness, we also list the total wave power (top), and the amount of wave power that can access the plasmasphere (bottom). The percentage of magnetic field wave power that exists in the $\theta$-$\phi$ region that can access the plasmasphere has been increased for all frequencies and source locations by considering this distribution width. However, these percentages remain extremely low, peaking at just 0.95% for $0.15 f_{ce}$ waves at $L = 5$. These results indicate that the distribution assumed in previous studies (e.g., Chen, Bortnik, et al., 2012a) likely resulted in overestimates of the wave power that can access the plasmasphere yet still required modest amplification inside of the plasmasphere to match observations. Assuming that ray-tracing is sufficiently realistic and the neglected nonplanar or small amplitude chorus waves do not play a role, the results of this analysis raise the question of how great an impact the chorus-to-hiss mechanism can have on the plasmaspheric hiss population as a whole, given the relatively low amount of chorus wave power that exists with the conditions required to access the plasmasphere.

One step that can increase the range of chorus wave normal angles that can access the plasmasphere is to consider an azimuthally asymmetric density model to account for the plasmaspheric plume/bulge on the duskside. This expansion in the range of wave normal angles that can access the plasmasphere is due to the increased azimuthal propagation that occurs in the presence of azimuthal density gradients. This effect may be interepreted, simply, as reducing the propagation distance between the wave source and the high-density plasmasphere. In the analysis presented here, we use the same density model as in Chen et al. (2009). This model (Jordanova et al., 2006; Rasmussen et al., 1993) is driven by the Rice Convection Model (RCM) electric field for the main phase of the 21 April 2001 storm. Additionally, wave damping rates outside the plasmasphere are explicitly calculated using the method of Bortnik et al. (2007), where analytical distribution functions were fit to suprathermal electron observations from the Combined Release and Radiation Effects Satellite (CRRES). Here we use the $AE > 300$ nT functions, since plume formation is typicaly associated with geomagnetically disturbed periods. Inside the plasmasphere, the model of Bell et al. (2002) is used. To study the effect of this asymmetric density, waves are injected from equatorial source locations at $L = 5, 6$, and MLT = 10, 12, 14, with frequencies of 0.10, 0.15, 0.20 $f_{ce}$ for the full range of wave vector orientations. We focus on 9 <MLT <15 as this is where azimuthal density gradients are strongest in this density model, and where higher power chorus waves exist based on statistical distributions (Li et al., 2011; Meredith et al., 2003, 2012). For MLT >15, azimuthal density gradients are present but chorus wave power is substantially lower. For MLT <9, high power chorus waves may be observed but the density model becomes approximately azimuthally symmetric, bringing results closer to those in Figure 1.

Figure 3a shows the azimuthally asymmetric density model, with wave injection locations indicated by white circles. Since this density model is MLT dependent, EMFISIS data are binned in 2-hr MLT wedges centered about the wave injection locations, in addition to sorting by L and frequency. The wave power spectral density is again modeled as a Gaussian distribution with a FWHM of $\Delta\theta = \Delta\phi = 20°$. The percentages of chorus wave power that can access the plasmasphere are shown in Figure 3b for all frequencies and source locations. The total occurrences, the total wave power, and the wave power that can access the plasmasphere are also provided. Sample cases of a $0.20 f_{ce}$ wave injected from $L = 5$ and MLT = 14, a $0.10 f_{ce}$ wave injected from $L = 6$ and MLT = 14, and a $0.15 f_{ce}$ wave injected from $L = 5$ and MLT = 12 are also shown. Figures 3c–3e show the wave vector orientations required for chorus waves to enter the plasmasphere (green area), and Figures 3f–3h show PDFs of wave power.

While the range of wave normal angles that can access the plasmasphere can be increased in the presence of azimuthal density gradients, we find the percentage of chorus wave power that can access the plasmasphere generally remains extremely low, ~1% or lower. The exception is when the chorus source is located in extremely close proximity to the plasmaspheric plume, and therefore azimuthal density gradients are strongest. In these cases, chorus with wave vectors that are initially approximately field-aligned are able to propagate into the plasmasphere as shown in Figures 3c and 3d. For the example case shown in Figures 3c and 3f with a source location right on the edge of the plume at MLT = 14 and $L = 5$ in this model, 82% of the measured chorus wave power is able to access the plasmasphere for $0.20 f_{ce}$ waves. This percentage is even higher for lower frequencies; 86% for $0.15 f_{ce}$ waves, and 94% for $0.10 f_{ce}$ waves.

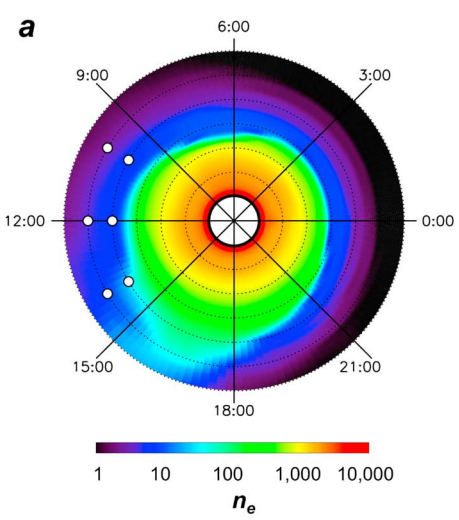


**b**

| Wave Power ($nT^2$) | | | | | | |
|---|---|---|---|---|---|---|
| | L = 5 | | | | | |
| | MLT = 10 | | MLT = 12 | | MLT = 14 | |
| 0.10 $f_{ce}$ | 0.0004% | 14,145<br>3.6 $nT^2$<br>$1.6x10^{-5}$ $nT^2$ | 0.16% | 16,559<br>1.4 $nT^2$<br>0.0023 $nT^2$ | 94% | 40,343<br>5.9 $nT^2$<br>5.6 $nT^2$ |
| 0.15 $f_{ce}$ | 0.020% | 10,999<br>7.2 $nT^2$<br>0.0015 $nT^2$ | 1.1% | 10,101<br>3.3 $nT^2$<br>0.036 $nT^2$ | 86% | 18,656<br>4.9 $nT^2$<br>4.3 $nT^2$ |
| 0.20 $f_{ce}$ | 0.037% | 13,664<br>8.9 $nT^2$<br>0.0033 $nT^2$ | 0.42% | 9,002<br>4.9 $nT^2$<br>0.020 $nT^2$ | 82% | 15,719<br>4.8 $nT^2$<br>3.9 $nT^2$ |
| | L = 6 | | | | | |
| | MLT = 10 | | MLT = 12 | | MLT = 14 | |
| 0.10 $f_{ce}$ | 0.034% | 49,321<br>6.2 $nT^2$<br>0.0021 $nT^2$ | 0% | 112,915<br>24 $nT^2$<br>0 $nT^2$ | 4.9% | 146,099<br>15 $nT^2$<br>0.74 $nT^2$ |
| 0.15 $f_{ce}$ | 0% | 42,096<br>23 $nT^2$<br>0 $nT^2$ | 0% | 69,541<br>18 $nT^2$<br>0 $nT^2$ | 0.0058% | 82,014<br>18 $nT^2$<br>0.0010 $nT^2$ |
| 0.20 $f_{ce}$ | 0% | 45,909<br>47 $nT^2$<br>0 $nT^2$ | 0% | 53,340<br>20 $nT^2$<br>0 $nT^2$ | 0.0013% | 55,348<br>17 $nT^2$<br>0.00023 $nT^2$ |

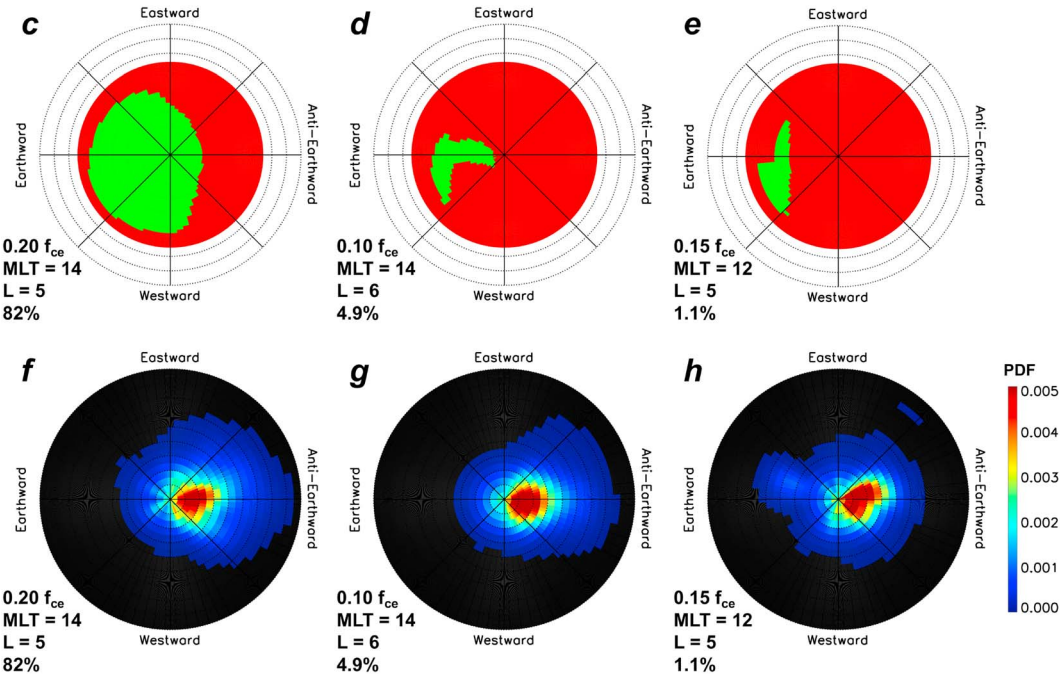


**Figure 3.** (a) Azimuthally asymmetric density model. (b) Percentages of wave power that can enter plasmasphere (left). Also provided (from top to bottom) are the occurrences, total wave power, and the wave power that can enter the plasmasphere. (c–e) The wave vector orientation required for waves to enter the plasmasphere. (f–h) Probability distribution functions of chorus wave power.

However, if the source location is moved radially outward away from the plume to $L = 6$, this percentage decreases rapidly such that only 4.9% of the observed chorus wave power exists with the conditions required to enter the plasmasphere at a frequency of $0.10f_{ce}$ (as shown in Figures 3d and 3g). Percentages are even lower for higher frequencies (much less than 1%). The same is true if the source location is moved azimuthally in MLT, the percentages drop substantially and are more in line with the results obtained when using an azimuthally symmetric density model. This is shown in Figures 3e and 3h for $0.15f_{ce}$ waves injected from a source at $L = 5$ and MLT = 12.

## 4. Conclusions

These results demonstrate that, on a global scale, chorus waves rarely exist with the wave vector orientation required to enter the plasmasphere, and the waves that are observed with the crucial $\theta$ and $\phi$ required to

propagate into the plasmasphere do not carry a substantial fraction of magnetic field wave power. In certain instances it is possible for a substantial fraction of chorus wave power to enter the plasmasphere in line with the chorus-to-hiss mechanism, but only from a spatially limited region close to the edge of a plasmaspheric plume, where azimuthal density gradients are strongest. As such, we conclude that strong azimuthal density gradients (such as those that occur on the edges of plumes) are actually a requirement if a significant fraction of chorus waves, and their associated chorus wave power, are to enter the plasmasphere and evolve into plasmaspheric hiss.

This result qualitatively indicates that the overall direct contribution of chorus to hiss may be small. This assessment is based on the fact that in the dawn region, where the statistical peak in chorus wave power is observed (e.g., Li et al., 2011; Meredith et al., 2003, 2012), the occurrence rate of plasmaspheric plumes is generally low (e.g., Darrouzet et al., 2008; Usanova et al., 2013) and therefore only a minimal fraction of chorus wave power exists with the wave vector orientation required to propagate into the plasmasphere. It is only in a small region close to the edge of plasmaspheric plumes, most frequently observed on the dusk side where the average chorus wave power has been observed to be significantly lower, that azimuthal density gradients are strong and it is possible for a substantial fraction of chorus wave power to enter the plasmasphere.

This analysis sheds new light on the chorus-to-hiss mechanism, highlighting that a direct one-to-one correspondence between chorus enhancements and plasmaspheirc hiss enhancements would only be observable for chorus waves that occur close to the edge of plasmaspheric plumes, which are most frequently observed in the post-noon and dusk sectors (Darrouzet et al., 2008; Usanova et al., 2013). For chorus waves outside of this small spatial region that are much less likely to experience the strong azimuthal density gradients associated with plumes, we conclude that minimal wave power can access the plasmasphere, and therefore chorus waves outside of this region offer only a negligible direct contribution to plasmaspheric hiss.

It is worth noting that the requirement for strong azimuthal density gradients in the form of plumes provides an explanation for the spatial structure observed by Agapitov et al. (2018), who found that correlation between chorus and hiss waves was observed most frequently between 12 and 16 MLT. This spatial limitation is also consistent with the direct observation of concurrent, or slightly delayed, enhancements between chorus and hiss measured between 13 and 17 MLT by Bortnik et al. (2009) and between 12 and 13 MLT by Li et al. (2015). Chorus wave power typically peaks on the dawn side (Li et al., 2011; Meredith et al., 2003, 2012), whereas plume occurrence peaks on the dusk side (Darrouzet et al., 2008; Usanova et al., 2013). The postnoon sector where the shoulders of these two statistical distributions overlap appears key for observing correlations between chorus and hiss.

The results of this study provide new perspective on the chorus-to-hiss mechanism and its spatial limitations, with the percentages reported in this study suggesting that it is unlikely that chorus waves directly provide a significant fraction of plasmaspheric hiss wave power and that additional mechanisms for amplifying and/or generating hiss (e.g., local instability and/or accumulating lightning whistlers) may be required (e.g., Santolík & Chum, 2009).

**Acknowledgments**
This work was performed under the support of JHU/APL contract 921647 under NASA Prime contract NAS5-01072. EMFISIS data may be obtained from the website (http://emfisis.physics.uiowa.edu/data/index). R. B. H. acknowledges the Natural Environment Research Council (NERC) Highlight Topic Grant NE/P01738X/1 (Rad-Sat). O. S. acknowledges support from grants LTAUSA17070 and GACR17-07027S and from the Praemium Academiae award.

## References

Agapitov, O., Mourenas, D., Artemyev, A., Mozer, F. S., Bonnell, J. W., Angelopoulos, V., et al. (2018). Spatial extent and temporal correlation of chorus and hiss: Statistical results from multipoint THEMIS observations. *Journal of Geophysical Research: Space Physics*, *123*, 8317–8330. https://doi.org/10.1029/2018JA025725

Angerami, J. J., & Thomas, J. O. (1964). Studies of planetary atmospheres: 1. The distribution of electrons and ions in the Earth's exosphere. *Journal of Geophysical Research*, *69*(21), 4537–4560. https://doi.org/10.1029/JZ069i021p04537

Bell, T. F., Inan, U. S., Bortnik, J., & Scudder, J. D. (2002). The Landau damping of magnetospherically reflected whistlers within the plasmasphere. *Geophysical Research Letters*, *29*(15), 1733. https://doi.org/10.1029/2002GL014752

Bingham, S. T., Mouikis, C. G., Kistler, L. M., Boyd, A. J., Paulson, K., Farrugia, C. J., et al. (2018). The outer radiation belt response to the storm time development of seed electrons and chorus wave activity during CME and CIR driven storms. *Journal of Geophysical Research: Space Physics*, *123*, 10,139–10,157. https://doi.org/10.1029/2018JA025963

Bortnik, J., Chen, L., Li, W., Thorne, R. M., & Horne, R. B. (2011). Modeling the evolution of chorus waves into plasmaspheric hiss. *Journal of Geophysical Research*, *116*, A08221. https://doi.org/10.1029/2011JA016499

Bortnik, J., Chen, L., Li, W., Thorne, R. M., Meredith, N. P., & Horne, R. B. (2011). Modeling the wave power distribution and characteristics of plasmaspheric hiss. *Journal of Geophysical Research*, *116*, A12209. https://doi.org/10.1029/2011JA016862

Bortnik, J., Chen, L., Li, W., Thorne, R. M., Nishimura, Y., Angelopoulos, V., & Kletzing, C. A. (2016). *Relationship between chorus and plasmaspheric hiss waves in low-frequency waves in space plasmas Edited by* A. Keiling, D.-H. Lee, & V. Nakariakov. Hoboken, NJ: John Wiley & Sons Inc. https://doi.org/10.1002/9781119055006.ch6

Bortnik, J., Li, W., Thorne, R. M., Angelopoulos, V., Cully, C., Bonnell, J., et al. (2009). An observation linking the origin of plasmaspheric hiss to discrete chorus emissions. *Science*, *324*(5928), 775–8. https://doi.org/10.1126/science.1171273

Bortnik, J., & Thorne, R. M. (2007). The dual role of ELF/VLF chorus waves in the acceleration and precipitation of radiation belt electrons. *Journal of Atmospheric and Solar-Terrestrial Physics*, *69*(3), 378–386. https://doi.org/10.1016/j.jastp.2006.05.030

Bortnik, J., Thorne, R. M., & Meredith, N. P. (2007). Modeling the propagation characteristics of chorus using CRRES suprathermal electron fluxes. *Journal of Geophysical Research*, *112*, A08204. https://doi.org/10.1029/2006JA012237

Bortnik, J., Thorne, R. M., & Meredith, N. P. (2008). The unexpected origin of plasmaspheric hiss from discrete chorus emissions. *Nature*, *452*(7183), 62–66. https://doi.org/10.1038/nature06741

Burtis, W. J., & Helliwell, R. A. (1969). Banded chorus a new type of VLF radiation observed in the magnetosphere by OGO 1 and OGO 3. *Journal of Geophysical Research*, *74*(11), 3002–3010. https://doi.org/10.1029/JA074i011p03002

Chen, L., Bortnik, J., Li, W., Thorne, R. M., & Horne, R. B. (2012a). Modeling the properties of plasmaspheric hiss: 1. Dependence on chorus wave emission. *Journal of Geophysical Research*, *117*, A05201. https://doi.org/10.1029/2011JA017201

Chen, L., Bortnik, J., Li, W., Thorne, R. M., & Horne, R. B. (2012b). Modeling the properties of plasmaspheric hiss: 2. Dependence on the plasma density distribution. *Journal of Geophysical Research*, *117*, A05202. https://doi.org/10.1029/2011JA017202

Chen, L., Bortnik, J., Thorne, R. M., Horne, R. B., & Jordanova, V. K. (2009). Three-dimensional ray tracing of VLF waves in a magnetospheric environment containing a plasmaspheric plume. *Geophysical Research Letters*, *36*, L22101. https://doi.org/10.1029/2009GL040451

Chen, L., Li, W., Bortnik, J., & Thorne, R. M. (2012). Amplification of whistler-mode hiss inside the plasmasphere. *Geophysical Research Letters*, *39*, L08111. https://doi.org/10.1029/2012GL051488

Chen, L., Thorne, R. M., Bortnik, J., Li, W., Horne, R. B., Reeves, G. D., et al. (2014). Generation of unusually low frequency plasmaspheric hiss. *Geophysical Research Letters*, *41*, 5702–5709. https://doi.org/10.1002/2014GL060628

Chum, J., & Santolík, O. (2005). Propagation of whistler-mode chorus to low altitudes: Divergent ray trajectories and ground accessibility. *Annales Geophysicae*, *23*, 3727–3738.

Darrouzet, F., De Keyser, J., Dcrau, P. M. E., El Lemdani Mazouz, F., & Vallires, X. (2008). Statistical analysis of plasmaspheric plumes with Cluster/WHISPER observations. *Annales de Geophysique*, *26*(8), 2403–2417.

Gurnett, D. A., & O'Brien, B. J. (1964). High latitude geophysical studies with satellite Injun 3: 5. Very low frequency electromagnetic radiation. *Journal of Geophysical Research*, *69*(1), 65–89. https://doi.org/10.1029/JZ069i001p00065

Hartley, D. P., Chen, Y., Kletzing, C. A., Denton, M. H., & Kurth, W. S. (2015). Applying the cold plasma dispersion relation to whistler mode chorus waves: EMFISIS wave measurements from the Van Allen Probes. *Journal of Geophysical Research: Space Physics*, *120*, 1144–1152. https://doi.org/10.1002/2014JA020808

Hartley, D. P., Kletzing, C. A., De Pascuale, S., Kurth, W. S., & Santolík, O. (2018). Determining plasmaspheric densities from observations of plasmaspheric hiss. *Journal of Geophysical Research: Space Physics*, *123*, 6679–6691. https://doi.org/10.1029/2018JA025658

Hartley, D. P., Kletzing, C. A., Kurth, W. S., Bounds, S. R., Averkamp, T. F., Hospodarsky, G. B., et al. (2016). Using the cold plasma dispersion relation and whistler mode waves to quantify the antenna sheath impedance of the Van Allen Probes EFW instrument. *Journal of Geophysical Research: Space Physics*, *121*, 4590–4606. https://doi.org/10.1002/2016JA022501

Hartley, D. P., Kletzing, C. A., Kurth, W. S., Hospodarsky, G. B., Bounds, S. R., Averkamp, T. F., et al. (2017). An improved sheath impedance model for the Van Allen Probes EFW instrument: Effects of the spin axis antenna. *Journal of Geophysical Research: Space Physics*, *122*, 4420–4429. https://doi.org/10.1002/2016JA023597

Hartley, D. P., Kletzing, C. A., Santolík, O., Chen, L., & Horne, R. B. (2018). Statistical properties of plasmaspheric hiss from Van Allen Probes observations. *Journal of Geophysical Research: Space Physics*, *123*, 2605–2619. https://doi.org/10.1002/2017JA024593

Horne, R. B. (1989). Path-integrated growth of electrostatic waves: The generation of terrestrial myriametric radiation. *Journal of Geophysical Research*, *94*(A7), 8895–8909. https://doi.org/10.1029/JA094iA07p08895

Inan, U. S., & Bell, T. F. (1977). The plasmapause as a VLF wave guide. *Journal of Geophysical Research*, *82*(19), 2819–2827. https://doi.org/10.1029/JA082i019p02819

Jordanova, V. K., Miyoshi, Y. S., Zaharia, S., Thomsen, M. F., Reeves, G. D., Evans, D. S., et al. (2006). Kinetic simulations of ring current evolution during the Geospace Environment Modeling challenge events. *Journal of Geophysical Research*, *111*, A11S10. https://doi.org/10.1029/2006JA011644

Kimura, I. (1966). Effects of ions on whistler-mode ray tracing. *Radio Science*, *1*, 269–284. https://doi.org/10.1002/rds196613269

Kletzing, C. A., Kurth, W. S., Acuna, M., MacDowall, R. J., Torbert, R. B., Averkamp, T., et al. (2013). The electric and magnetic field instrument suite and integrated science (EMFISIS) on RBSP. *Space Science Reviews*, *179*, 127–181. https://doi.org/10.1007/s11214-013-9993-6

Li, W., et al. (2013). An unusual enhancement of low-frequency plasmaspheric hiss in the outer plasmasphere associated with substorm-injected electrons. *Geophysical Research Letters*, *40*, 3798–3803. https://doi.org/10.1002/grl.50787

Li, W., Bortnik, J., Thorne, R. M., & Angelopoulos, V. (2011). Global distribution of wave amplitudes and wave normal angles of chorus waves using THEMIS wave observations. *Journal of Geophysical Research*, *116*, A12205. https://doi.org/10.1029/2011JA017035

Li, W., Chen, L., Bortnik, J., Thorne, R. M., Angelopoulos, V., Kletzing, C. A., et al. (2015). First evidence for chorus at a large geocentric distance as a source of plasmaspheric hiss: Coordinated THEMIS and Van Allen Probes observation. *Geophysical Research Letters*, *42*, 241–248. https://doi.org/10.1002/2014GL062832

Li, W., Mourenas, D., Artemyev, A. V., Agapitov, O. V., Bortnik, J., Albert, J. M., et al. (2014). Evidence of stronger pitch angle scattering loss caused by oblique whistler-mode waves as compared with quasi-parallel waves. *Geophysical Research Letters*, *41*, 6063–6070. https://doi.org/10.1002/2014GL061260

Li, W., Santolik, O., Bortnik, J., Thorne, R. M., Kletzing, C. A., Kurth, W. S., & Hospodarsky, G. B. (2016). New chorus wave properties near the equator from Van Allen Probes wave observations. *Geophysical Research Letters*, *43*, 4725–4735. https://doi.org/10.1002/2016GL068780

Lyons, L. R., & Thorne, R. M. (1973). Equilibrium structure of radiation belt electrons. *Journal of Geophysical Research*, *78*(13), 2142–2149. https://doi.org/10.1029/JA078i013p02142

Lyons, L. R., Thorne, R. M., & Kennel, C. F. (1972). Pitch-angle diffusion of radiation belt electrons within the plasmasphere. *Journal of Geophysical Research*, *77*(19), 3455–3474. https://doi.org/10.1029/JA077i019p03455

Malaspina, D. M., Jaynes, A. N., Hospodarsky, G., Bortnik, J., Ergun, R. E., & Wygant, J. (2017). Statistical properties of low frequency plasmaspheric hiss. *Journal of Geophysical Research: Space Physics*, *122*, 8340–8352. https://doi.org/10.1002/2017JA024328

Mauk, B. H., Fox, N. J., Kanekal, S. G., Kessel, R. L., Sibeck, D. G., & Ukhorskiy, A. (2012). Science objectives and rationale for the Radiation Belt Storm Probes mission. *Space Science Reviews*, *179*, 3–27. https://doi.org/10.1007/s11214-012-9908-y

Meredith, N. P., Horne, R. B., Bortnik, J., Thorne, R. M., Chen, L., Li, W., & Sicard-Piet, A. (2013). Global statistical evidence for chorus as the embryonic source of plasmaspheric hiss. *Geophysical Research Letters*, *40*, 2891–2896. https://doi.org/10.1002/grl.50593

Meredith, N. P., Horne, R. B., Sicard-Piet, A., Boscher, D., Yearby, K. H., Li, W., & Thorne, R. M. (2012). Global model of lower band and upper band chorus from multiple satellite observations. *Journal of Geophysical Research*, *117*, A10225. https://doi.org/10.1029/2012JA017978

Meredith, N. P., Horne, R. B., Thorne, R. M., & Anderson, R. R. (2003). Favored regions for chorus-driven electron acceleration to relativistic energies in the Earth's outer radiation belt. *Geophysical Research Letters*, *30*(16), 1871. https://doi.org/10.1029/2003GL017698

Meredith, N. P., Horne, R. B., Thorne, R. M., Summers, D., & Anderson, R. R. (2004). Substorm dependence of plasmaspheric hiss. *Journal of Geophysical Research*, *109*, A06209. https://doi.org/10.1029/2004JA010387

Ni, B., Li, W., Thorne, R. M., Bortnik, J., Ma, Q., Chen, L., et al. (2014). Resonant scattering of energetic electrons by unusual low-frequency hiss. *Geophysical Research Letters*, *41*, 1854–1861. https://doi.org/10.1002/2014GL059389

Rasmussen, C. E., Guiter, S. M., & Thomas, S. G. (1993). A two dimensional model of the plasmasphere: Refilling time constants. *Planetary and Space Science*, *41*, 35–43. https://doi.org/10.1016/00320633(93)90015T

Santolík, O., & Chum, J. (2009). The origin of plasmaspheric hiss. *Science*, *324*(5928), 729–730. https://doi.org/10.1126/science.1172878

Santolík, O., Chum, J., Parrot, M., Gurnett, D. A., Pickett, J. S., & Cornilleau-Wehrlin, N. (2006). Propagation of whistler mode chorus to low altitudes: Spacecraft observations of structured ELF hiss. *Journal of Geophysical Research*, *111*, A10208. https://doi.org/10.1029/2005JA011462

Santolík, O., Parrot, M., & Lefeuvre, F. (2003). Singular value decomposition methods for wave propagation analysis. *Radio Science*, *38*(1), 1010. https://doi.org/10.1029/2000RS002523

Santolík, O., Pickett, J. S., Gurnett, D. A., & Storey, L. R. O. (2002). Magnetic component of narrow-band ion cyclotron waves in the auroral zone. *Journal of Geophysical Research*, *107*(A12), 1444. https://doi.org/10.1029/2001JA000146

Selesnick, R. S., Blake, J. B., & Mewaldt, R. A. (2003). Atmospheric losses of radiation belt electrons. *Journal of Geophysical Research*, *108*(A12), 1468. https://doi.org/10.1029/2003JA010160

Summers, D., Ni, B., & Meredith, N. P. (2007). Timescales for radiation belt electron acceleration and loss due to resonant waveparticle interactions: 2. Evaluation for VLF chorus, ELF hiss, and electromagnetic ion cyclotron waves. *Journal of Geophysical Research*, *112*, A04207. https://doi.org/10.1029/2006JA011993

Taubenschuss, U., & Santolík, O. (2019). Wave polarization analyzed by singular value decomposition of the spectral matrix in the presence of noise. *Surveys in Geophysics*, *40*, 39. https://doi.org/10.1007/s10712-018-9496-9

Thorne, R. M. (2010). Radiation belt dynamics: The importance of waveparticle interactions. *Geophysical Research Letters*, *37*, L22107. https://doi.org/10.1029/2010GL044990

Thorne, R. M., Li, W., Ni, B., Ma, Q., Bortni, J., Baker, D. N., et al. (2013). Evolution and slow decay of an unusual narrow ring of relativistic electrons near l-3.2 following the September 2012 magnetic storm. *Geophysical Research Letters*, *40*, 3507–3511. https://doi.org/10.1002/grl.50627

Thorne, R. M., Smith, E. J., Burton, R. K., & Holzer, R. E. (1973). Plasmaspheric hiss. *Journal of Geophysical Research*, *78*(10), 1581–1596. https://doi.org/10.1029/JA078i010p01581

Usanova, M. E., Darrouzet, F., Mann, I. R., & Bortnik, J. (2013). Statistical analysis of EMIC waves in plasmaspheric plumes from Cluster observations. *Journal of Geophysical Research: Space Physics*, *118*, 4946–4951. https://doi.org/10.1002/jgra.50464

Wang, C., Zong, Q., Xiao, F., Su, Z., Wang, Y., & Yue, C. (2011). The relations between magnetospheric chorus and hiss inside and outside the plasmasphere boundary layer: Cluster observation. *Journal of Geophysical Research*, *116*, A07221. https://doi.org/10.1029/2010JA016240

Xiao, F., et al. (2015). Wave-driven butterfly distribution of Van Allen belt relativistic electrons. *Nature Communications*, *6*, 8590. https://doi.org/10.1038/ncomms9590

Xiao, F., Liu, S., Tao, X., Su, Z., Zhou, Q., Yang, C., et al. (2017). Generation of extremely low frequency chorus in Van Allen radiation belts. *Journal of Geophysical Research: Space Physics*, *122*, 3201–3211. https://doi.org/10.1002/2016JA023561

Xiao, F., Su, Z., Zheng, H., & Wang, S. (2009). Modeling of outer radiation belt electrons by multidimensional diffusion process. *Journal of Geophysical Research*, *114*, A03201. https://doi.org/10.1029/2008JA013580

Xiao, F., Su, Z., Zheng, H., & Wang, S. (2010). Three-dimensional simulations of outer radiation belt electron dynamics including cross-diffusion terms. *Journal of Geophysical Research*, *115*, A05216. https://doi.org/10.1029/2009JA014541

Zhou, Q., Xiao, F., Yang, C., Liu, S., He, Y., Wygant, J. R., et al. (2016). Evolution of chorus emissions into plasmaspheric hiss observed by Van Allen Probes. *Journal of Geophysical Research: Space Physics*, *121*, 4518–4529. https://doi.org/10.1002/2016JA022366